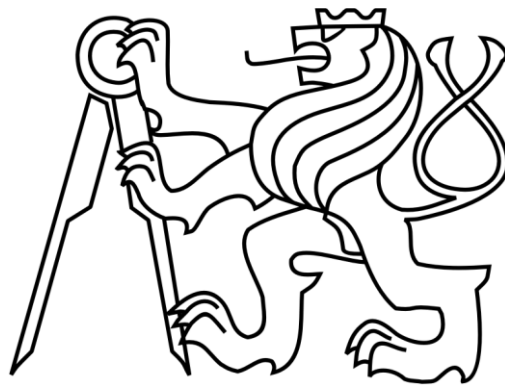


CZECH TECHNICAL UNIVERSITY IN PRAGUE
FACULTY OF CIVIL ENGINEERING
Department of Mechanics



BACHELOR THESIS

**Investigation of Aggregate Influence on
Fracture Properties of Mortars by FEA**

Jakub Antoš

2013

Supervisor: Jan Zeman

Honesty Declaration

I declare that this bachelor thesis has been carried out by me and only with the use of materials that are stated in the literature sources. The results contained in the thesis were also presented on the conference Engineering Mechanics 2013.

March 19, 2013

Jakub Antoš

.....

Acknowledgement

I would like to thank my supervisors, Václav Nežerka and Jan Zeman, who supported me, introduced me to the issues of numerical modeling and explained me patiently everything I needed. I would also like to thank my parents who supported me not only during the thesis but during the whole studies.

Abstract

Virtual testing of composite materials is, compared to a conventional experimental analysis, less time consuming, and it can very clearly reveal the failure mode. Therefore, it can be used for an optimization of the shape and amount of aggregates. Unlike the basic analytical homogenization methods, numerical modeling can predict the strength of the material and energy needed for the crack propagation. In our study three-point bending and splitting tests, by means of 2D plane-stress nonlinear finite element analysis utilizing isotropic damage model, were simulated. There were two types of aggregates investigated by the study - sand and crushed bricks. The sand particles were considered as round, angular or having the shape of ellipsoids, while the crushed brick particles were only of an angular shape. The results of the analysis indicate that angular aggregates of bigger size contribute to an increased fracture energy of the mortars, while the mortars containing fine round aggregates exhibit higher strength due to absence of stress concentrations around the grains. When the sand particles are replaced by much more compliant crushed brick particles, the mortar is able to sustain much bigger deformation within the elastic region.

Keywords: FEM, damage model, mortar, three point bending test, splitting test, crushed bricks, fracture energy

Abstrakt

Virtuální testování s využitím numerických metod, v porovnání s konvenční experimentální analýzou, vyžaduje mnohem méně času a přesto je schopné nám přesně odhalit mechanismus poškození. Proto může být snadno použit pro optimalizaci tvaru a množství kameniva. Na rozdíl od základních analytických homogenizačních metod, může numerické modelování předpovědět pevnost materiálu a energii potřebnou ke vzniku a šíření trhliny. Naše testy - tří bodový ohyb a test rozštěpení, byly virtuálně prováděny nelineárním výpočtem pomocí 2D rovinné napjatosti metodou konečných prvků využívající izotropický model poškození. Testovány byly dva druhy plniva - písek a drcené cihly. Výsledky analýzy ukazují, že ostrohranné kamenivo větších velikostí přispívá ke zvýšení lomové energie malt, zatímco malty obsahující jemné kulové tvary kameniva vykazují vyšší pevnost v důsledku snížení koncentrace napětí kolem zrn. Použití drcených cihel, jako plniva místo písku, má za následek větší mezní elastickou deformaci.

Klíčová slova: MKP, model poškození, malty, tříbodový ohyb, štěpení klínem, drcená cihla, lomová energie

Contents

Introduction.....	8
Goals	9
PART I: THEORETICAL BACKGROUND	10
1 Finite Element Method.....	11
1.1 Historical Background.....	11
1.2 State of Art.....	12
1.2.1 Present Software Packages	12
1.3 Principle of FEM	13
1.3.1 Discrete Elements - 1D	14
1.3.2 Continuum Elements - 2D and 3D	14
1.3.2.1 Simplex, Complex and Multiplex Elements	15
1.3.3 Convergence Conditions	16
1.3.4 Element Aspect Ratio	16
1.3.5 Limitations of FEM.....	17
1.3.6 Linearity / Nonlinearity	17
1.3.6.1 Concept of Time Curves	18
1.3.6.2 Full Newton-Raphson Method.....	19
2 Summary of the Theory of Elasticity.....	21
2.1 Strain-to-Displacement Relations.....	21
2.1.1 Displacements	21
2.1.2 Strains	22
2.2 Static Equations	22
2.3 Constitutive Equations	23
2.3.1 Principal Stresses	24
2.3.2 Plane-Stress.....	25
2.3.3 Plane-Strain.....	26
3 Damage Model.....	27
3.1 Isotropic Damage Model	27
3.2 Material Softening	28
3.2.1 Linear Softening.....	28
3.2.2 Exponential Softening.....	29
3.2.3 Damage Localization.....	30
PART II: CALCULATIONS	31
4 Calculations	32
4.1 Steps of Calculation.....	32
4.2 Geometry of Tested Specimens	32
4.2.1 Principles Used for Generation of Aggregates.....	34

4.3	Finite Element Calculation.....	34
4.3.1	Summary of Tested Specimens.....	35
4.4	Stress-strain Diagrams.....	36
4.5	Postprocessing	38
5	Results and Discussion	39
5.1	Bending Test.....	39
5.2	Splitting Test	41
	Conclusion	43
	References	44

Introduction

It has been observed by many [1, 2] that the material properties of mortars and concrete are dependent on the amount, type and geometry of aggregates in the mix. The first purpose of this work is to investigate the influence of the aggregate shape and size on the mechanical properties of mortars, composed of sand aggregates and a brittle matrix. Namely, the influence of aggregates on flexural strength of the tested mortar was determined from a three-point bending test simulations, while the fracture energy was evaluated from simulations of a splitting test.

The second purpose is to investigate the role of crushed bricks particles within the mortar under the mechanical loading. Lime-based mortars were widely used in ancient times and they find they use nowadays for the purposes of cultural heritage restoration. These mortars were traditionally composed of air-slaked lime, pozzolans and sand aggregates. Phoenicians were probably the first ones to add also the fragments of crushed bricks or pottery into their mortars [3] and the technology was later adopted by the Romans who used these mortars especially in baths and aqueducts. One reason could have been to increase the hydraulicity of the mortars [2], but the hydraulic reactions on the lime-crushed brick interface is relatively weak to significantly enhance the mechanical properties. Namely, numerous simulations of three-point bending and splitting tests were carried out, in order to investigate the fracture mechanical properties of the samples, stress concentrations around various aggregate types and to observe the failure mechanism. Computationally less demanding analytical homogenization methods used e.g. in [4] for an investigation of mortars containing crushed brick particles cannot reveal the failure and post-peak behavior.

The first part of this work provides a theoretical background of the FE calculations, non-linear material behavior and basics of theory of elasticity. In the second part the tested specimens are described with all steps of the calculations, and the results are presented and discussed.

Goals

The main goal of this thesis is to learn basics principles of FE calculations used in a practice of civil engineer. In particular, the main goals of the thesis are to:

- study the historical evolution of FEM leading to numerical simulations used in FE nowadays
- study the principles of FEM
- study the non-linear behavior of composite materials
- study the damage model for the needs of simulations
- investigate the influence of shape of the sand particles on fracture properties
- investigate the influence of crushed bricks used instead of sand aggregates on the fracture properties

PART I:
THEORETICAL
BACKGROUND

1 Finite Element Method

The finite element method (FEM) is one of the most important numerical methods for solving physical phenomena in encountered engineering nowadays. In particular, it is widely used if the phenomena or their parts can be described by partial differential equations, since solving these equations by classical analytical methods for arbitrary shapes is impossible. However, the finite element method is a numerical approach by which the partial differential equations can be solved approximately.

1.1 Historical Background

The origins of FEM can be traced back to the first half of the 20th century. Mathematicians discovered in 1943 paper by R. Courant (1943), in which he used triangular elements with variational principles to solve vibration problems. Many mathematicians say that it was the discovery of the method. Other important persons who have significantly contributed to develop the method were: M. J. Turner, R. W. Clough, E. L. Wilson, K. J. Bathe, J. H. Argyris, T. Belytschko, O. Zienkiewicz. In the first years, FEM lacked theoretical basis and many engineers did not believe, that results provided by FEM can give the right solution.

In the late 1960s, field of interest around FEM rose up rapidly; Edward L. Wilson developed one of the first FEM computing program. This program was marked as "freeware" in today's terminology, which was very common in the early 1960's, because there were not any commercial interests from the beginning. The program could work only with two-dimensional stress analysis, and it was used by many academic groups and industrial laboratories to demonstrate the power and versatility of finite elements.

Later on, in 1965, NASA funded a project to develop a program for general-purpose finite element analysis. The program was known as NASTRAN. It should be noted that in 1965-1980 there was The Third Generation of operating systems. Despite its enormous size and problems, OS/360 and similar third-generation operating systems were sufficient for the needs of computing [5]. NASTRAN was developed for the needs of aeronautics. It was able to work e.g. with two- and three-dimensional stress analysis, shell and beam elements, it could analyze complex structures, such as airframes, or analysis of dynamics problems. First version was intended for public use, but unfortunately it had many bugs [6]. After the completion of the program and debugging, the program was marketed to the industry. In 1990, the program was the workhorse of most large industrial firms and a \$100 million worth business.

At nearly the same time, a finite element program at Westinghouse Electronics Corp, primarily used for the analysis of nuclear reactors, was developed. In 1969 it was released to market and called ANSYS. The program had both - linear and nonlinear options, and it was soon widely use in many companies. In 1996 ANSYS went public and in 2006 it was worth \$1.8 billion.

Another, and probably the last important representative of FEM programs is ABAQUS. ABAQUS was developed by a company called HKS, which was founded in 1978. The program was focused on nonlinear analysis from the beginning, but later the linear capabilities were also added. This program was widely used by researchers because HKS introduced gateways to the program core, so that users could add own new material models and elements. In 2005, the company was sold for \$413 million [6].

Many non-commercial software have been also developed, providing the users with sourcefiles, but offering minimum graphical interface. These programs, such as OOFEM [7], find their place mainly in research.

1.2 State of Art

FEM is absolutely indispensable in today's world. It isn't used only in the aeronautics industry like in the early 60's. Nowadays, we are not limited by the computational power and more sophisticated models can be done. Usage of FEM is too wide to list, here are a few examples to provide a clue about its versatility:

- stress and thermal analyses of industrial parts such as pipes, electronics chips, automotive engines and aircraft;
- seismic analysis of dams, power plants, cities and high-rise buildings;
- dynamics problems - in civil engineering and other branches of industry;
- fluid flow analysis, determining the flow of pollutants and contaminants, and air in ventilation systems;
- electromagnetic analysis of antennas, transistors and aircraft signatures;
- analysis of surgical procedures such as plastics surgery, jaw reconstruction and many others.

However, this is a very short brief and new areas of application are constantly emerging. This thesis is focused on the usage of FEM in structural mechanics.

1.2.1 Present Software Packages

In present (2013) there are many software packages on the market. List below shows the most used software packages. The list is sorted according to their use.

- *Universal* - ANSYS, MSC.Nastran, MSC.Narc, ABAQUS, Adina, Cosmos/M, Systus, OOFEM, ...
- *Specialized* - MSC.Superform, MSC.Superforge, Antares, Sysweld, Franc3D, PAM Stamp, PAM Crash, ...
- *pre and post processors* - Hyperworks, MSC.Patran, Femap, Enight, ...
- *integrated in CAD systems* - I-DEAS, Catia, Pro/E, Autodesk Inventor, Autodesk Revit, ...

This is one point of view. The second can be divided into categories according to the license. There are two major categories of software packages:

- Free/Open source - OOFEM, FEBio, Code Aster, CalculiX, ...
- Commercial - ANSYS, ABAQUS, ADINA, LS-DYNA, ...

Reader can find the full list here [8].

1.3 Principle of FEM

The finite element method was developed as a matrix method of structural analysis. Firstly, it was used for trusses and frames, we call them discrete structures. Later it was extended for continuum structures.

FEM method is based on conventional theory of elasticity (force equilibrium and compatibility of displacements), variational principles, and energy theorems. This method produces a huge package of simultaneous equations in most cases. These equations represent relationship between load and displacement. This is the reason why this method is suited for matrix calculus and its growth was initiated by the development of computers.

The FEM model contains finite a number of **elements** connected at points called **nodes** as shown on Figure 1

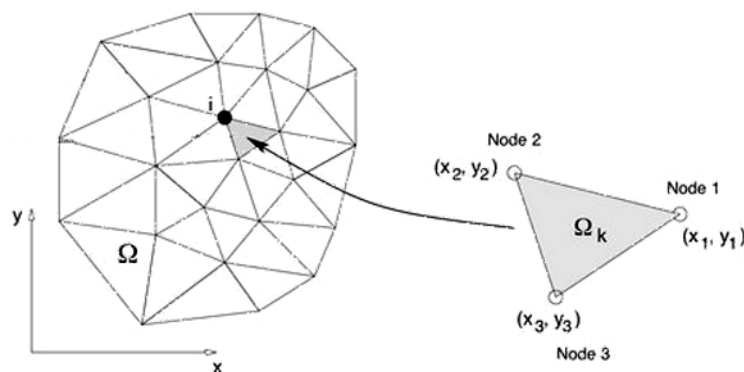


Figure 1 - Meshed model Ω by triangular elements.

FEM is an extension of Rayleigh-Ritz method, eliminating the difficulty of dealing with a large polynomial representing a suitable displacement field valid over the entire structure [6]. Cornerstone of this method consists in choosing a displacement field over the entire component, usually in the form of a polynomial function, and evaluating unknown coefficients of the polynomial for minimum potential energy. FEM approach, based on minimum potential energy theorem, converges to the correct solution from a higher value as the number of elements in the model increase. It gives an approximate solution. That is the reason why we call FEM one of the method of approximation [6]. The number of elements used in model is selected by the engineer, based on the required accuracy of solution as well as the computing power available. This model has an assumed behavior or response of each element to the set applied loads, and evaluating the unknown field variable (displacement, temperature) at these finite number of nodes.

1.3.1 Discrete Elements - 1D

A truss structure, as shown on Figure 2, consists of a collection of slender elements, called bars. Nodes are chosen at the connection of two or more discrete elements, at junction of two different materials, or at a point of load application. We call them discrete structures. In the 1-D element, the axial dimension is very large in comparison with the cross-section dimensions, and load is assumed to act uniformly over the entire cross-section. This clearly reflects that the solution (displacement) is taken as a function of x , along the axis of the element. Stress and strain are uniform entire the cross-section too. The solution obtained in most of these cases, is exact.



Figure 2 - Typical truss structure: Forth Rail Bridge (*1890), United Kingdom.

The only internal forces are those in axial direction. Strains in the element are obtained as derivatives of the displacement polynomial, and are thus they are expressed in terms of the nodal displacements. Stresses are expressed in terms of strains, using the appropriate stress-strain relationship. By equating work done by the external forces to the change in internal strain energy of the element and applying variational principle, load-displacement relationships of the element in terms of stiffness coefficients are obtained. They represent a system of simultaneous equations relating the nodal loads to the nodal displacements [6].

1.3.2 Continuum Elements - 2D and 3D

When one of the cross sectional dimensions, width is significant compared to the length of the member while the thickness is very small, it is considered as a 2-D element. Displacement variation is therefore neglected across the thickness. This means that we neglect the third dimension - the thickness. We consider that the load is applied to be acting in the plane of the element, along the X-direction or/and Y-direction. This element has a two degrees of freedom per node - displacement along X and Y directions. Load along X-direction produces lateral strain and, hence, a displacement u_y in the Y-direction v (because of Poisson's effect). Thus, displacements u_x and u_y are functions of x and y coordinates of the point [9].

In the case of continuum, which is modeled by 2-D respectively 3-D elements, there is no unique finite element model for analysis. Each engineer may use a particular number of nodes and a particular orientation of elements. That means that results provided by FEM obtained by different engineers may be vary. This may be a problem. The results obtained by FEM have to be suitably modified for compliance with mandatory safety codes. Varying number or type of elements, but at a higher computational cost, may improve accuracy.

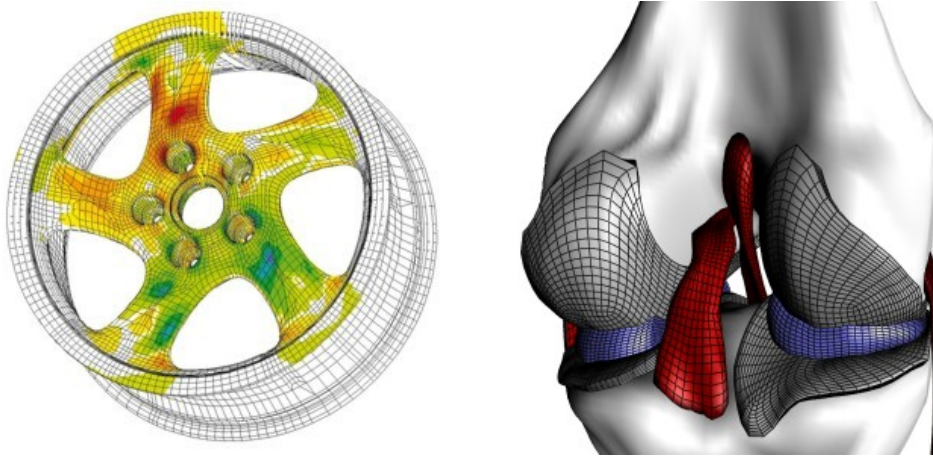


Figure 3 - Examples of continuous meshed models.

1.3.2.1 Simplex, Complex and Multiplex Elements

Finite elements can be classified into three categories.

- *Simplex* elements are those obtained by joining $n+1$ nodes in n -dimensional space. Approximating function of displacements consists of only constant terms and linear terms, if nodal DOFs include only translational modes [6].
- *Complex* elements are those elements whose displacement function consists of quadratics, cubic, or higher order terms. The complex elements may have the same shape as a simplex elements but will have additional boundary and, sometimes, internal nodes [9]. For example quadratic models like 6-noded triangular element and 10-noded tetrahedron element.
- *Multiplex* elements are those elements whose boundaries are parallel to the coordinate axes and whose displacement function consists of higher order terms. For example 4-noded rectangle element (2D) or 8-noded hexahedron element (3D).

Examples of the basics elements are shown in Figure 4, classified by their dimension.

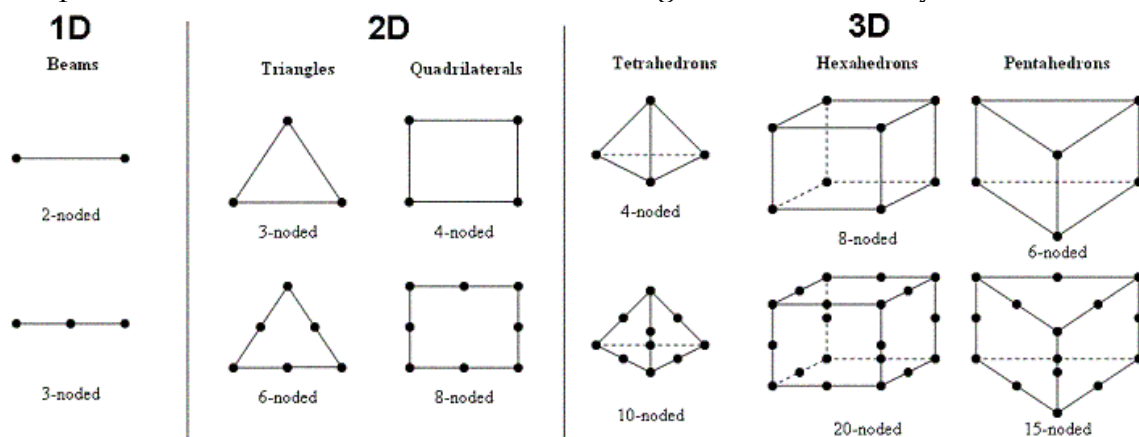


Figure 4 - Basics elements used in FEM.

1.3.3 Convergence Conditions

While we choose a function that represents displacements at any point of the element, it should be ensured, that several convergence conditions are satisfied.

- The function should be continuous and differentiable (to obtain e.g. strains) within the element.
- The displacement polynomial should include constant term, representing e.g. rigid body displacement in solid mechanics.
- The polynomial should include linear terms, which on differentiation give constant terms.
- Compatibility of the displacement and its derivatives, up to the required order, must be satisfied across inter-element boundaries. Otherwise the displacement solution may result in separated or overlapped inter-element boundaries when the displacement patterns of deformed elements with a common boundary are plotted separately.
- The polynomial shall satisfy geometric isotropy.

This list of convergence conditions was taken from the book [6].

1.3.4 Element Aspect Ratio

Certain conditions are generally specified in the standard packages on the sizes and included angles for various elements. Aspect ratio is defined for this purpose as the ratio of the longest side to the shortest one. It is usually limited to 5, while the included angle is usually limited to 45° to 135° for a triangular element and to 60° to 120° for a quadrilateral or 3-D elements. A few examples of 2-D elements with valid and invalid shapes are shown in Figure 5 [6].

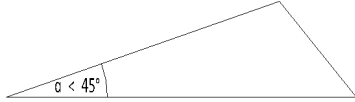
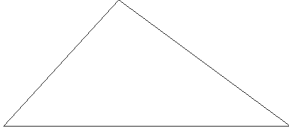
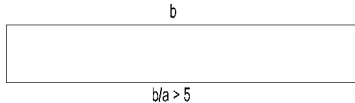


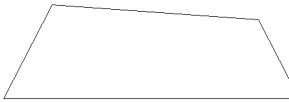
undesirable shapes of elements	preferred shapes of elements
	
	
	

Figure 5 - Undesirable and preferred shapes of elements.

1.3.5 Limitations of FEM

Finite element method is very versatile and powerful and it can enable designers to obtain information about the behavior of complicated structures with almost arbitrary shape and loading. In spite of the significant advances that have been made during developing the finite element packages, the results obtained must be carefully examined before they can be used. The most significant limitation of finite element method is that the accuracy of the obtained solution is usually a function of the mesh resolution. Any regions of highly concentrated stress, such as around loading points and supports, must be carefully analyzed with the use of a sufficiently refined mesh.

Because of singularities and some other phenomena encountered in the calculations, the results must be interpreted by a seasoned engineer. Special care must be taken to analyze some problems. An additional concern for any user is that because current packages can solve so many sophisticated problems, there is a strong temptation to "solve" problems without doing the hard work of thinking through them and understanding the underlying mechanics or other physical applications.

Obtaining solutions using FEM often requires substantial amounts of computational cost and time. Nevertheless, finite element packages have become increasingly indispensable to mechanical design and analysis [10].

1.3.6 Linearity / Nonlinearity

Linear analysis is based on linear relationship between stress and strain or strains and displacements. This analysis is used when the stress at any point is below the elastics limit and Hooke's law is valid. Results obtained for individual load combinations can be summed together, because there is a validity of linear superposition.

The non-linear analysis may be needed when dealing with the shape or material nonlinearity, or there can be some boundary nonlinearities. For example aircraft wing with large deflections due to applied loads, belongs to the category of geometrical nonlinearity. In solving these problems, geometry of every component must be redefined after every load step by adding the displacements at various nodes to the nodal coordinates, for defining the true geometry to be used for the next load step [11].

From the another point of view, the material may exhibit nonlinear stress-strain relationship, such as in case of plasticity or damage. This represents the category of material nonlinearity. During the nonlinear analysis, the total load must be applied in small steps, in which we assume a linear behavior. The most frequent boundary nonlinearities are encountered in contact problems, a typical boundary nonlinear problem is supporting by means of Winkler-Pasternak soil model [12].

Consequences of nonlinear structural behavior that have to be recognized are [13]:

- The principle of superposition cannot be applied. Therefore, the results of several load cases cannot be combined, and cannot be scaled.

- The history of loading is important. Especially, in case of plastic behavior of the material. This is accomplished by dividing loads into small increments in nonlinear FE analysis.
- The structural behavior can be significantly non-proportional to the applied load.
- The initial state of stress (e.g. in concrete - residual stresses from shrinkage or in metals - residual stresses due to welding) may be important.

1.3.6.1 Concept of Time Curves

As stated above, in nonlinear static analysis, the loads are applied in incremental steps using time curves. The "time" doesn't mean real time, but represents pseudo time, which denotes the intensity of the applied loads at certain step.

Discretized weak form of the governing equations for linear task is

$$\mathbf{K}\mathbf{d} = \mathbf{f}_{\text{ext}} \quad (1.01)$$

where \mathbf{K} is the stiffness matrix, \mathbf{d} is the displacement matrix vector¹, and \mathbf{f}_{ext} vector of nodal loads representing from the surface and volume forces. We can rewrite equation (1.01) as

$$\mathbf{f}_{\text{int}} = \mathbf{f}_{\text{ext}} \quad (1.02)$$

where \mathbf{f}_{int} is the vector of nodal forces equivalent stress acting in the elements. If the solved problem contains some structural nonlinearity, then the relationship between global vectors of nodal forces and nodal displacements is nonlinear:

$$\mathbf{f}_{\text{int}}(\mathbf{d}) = \mathbf{f}_{\text{ext}} \quad (1.03)$$

The task can be solved separately for individual time (load) steps. Assume that the solution in step t is known, for example from the previous calculation. After incremental change of load we can write

$$\mathbf{f}_{\text{int}}(\bar{\mathbf{d}} + \Delta\mathbf{d}) = \bar{\mathbf{f}}_{\text{ext}} + \Delta\mathbf{f}_{\text{ext}} \quad (1.04)$$

Vector $\bar{\mathbf{f}}_{\text{ext}} + \Delta\mathbf{f}_{\text{ext}}$ is known, while the increment of displacements $\Delta\mathbf{d}$ needs to be calculated to meet (at least approximately) governing equations (1.04). Because of the non-linear relationship between \mathbf{f}_{int} and $\mathbf{f}_{\text{ext}}(\mathbf{d})$ the vector of internal forces \mathbf{f}_{int} cannot be generally found analytically. There have been developed several numerical method to solve these problems:

- Solutions without an incremental iterations (Euler method).
- Iterative solution based on the Newton-Raphson method.
- Other iterative methods, such as BFGS (Broyden-Fletcher-Goldfarb-Shann).

¹ Here the vector has no physical meaning with respect to coordinate system, but it is just an array of values in individual nodes.

In our calculations, the Newton-Raphson method was used, for more details see the following sections.

1.3.6.2 Full Newton-Raphson Method

Newton-Raphson (NR) method, sometimes called tangent method, is an iterative numerical method used for solving the systems of nonlinear equations. NR method is referred to as the method of the tangents, because the solution of the equation $f(x) = 0$ is sought in the direction of the tangent function $f(x)$. Using the incremental step-by-step analysis. Knowing that we can rewrite (1.04) as a

$$\mathbf{K}(\mathbf{d})\Delta\mathbf{d} = \bar{\mathbf{f}}_{\text{ext}} - \mathbf{f}_{\text{int}}(\mathbf{d}) \quad (1.05)$$

where $\mathbf{K}(\mathbf{d})$ is the stiffness matrix, relating the loading increments to the increments of deformation, and \mathbf{d} are the initial deformations, obtained the previous step. The right side of the of the equation (1.05) represents out-of-balance forces due to the load increment, i.e. total load level after applying the load increment minus forces at the end of the previous load step. General rule is that the stiffness matrix \mathbf{K} is deformation depended as a function of \mathbf{d} , but it is usually ignored within a load increment to preserve the linearity. In our case, the stiffness matrix is calculated based on the value of \mathbf{d} related to the level before the load increment. The nonlinearity of equation (1.05) introduces a nonlinearity of internal forces:

$$\mathbf{f}_{\text{int}}(\alpha\mathbf{d}) \neq \alpha\mathbf{f}_{\text{int}}(\mathbf{d}) \quad (1.06)$$

where α is an arbitrary constant, and the non-linearity can be also illustrated on the stiffness matrix, because

$$\mathbf{K}(\mathbf{d}) \neq \mathbf{K}(\mathbf{d} + \Delta\mathbf{d}) \quad (1.07)$$

We can rewrite (1.05) for the i -th iteration

$$\mathbf{K}(\mathbf{d}_{i-1})\Delta\mathbf{d}_i = \bar{\mathbf{f}}_{\text{ext}} - \mathbf{f}_{\text{int}}(\mathbf{d}_{i-1}) \quad (1.08)$$

all $\mathbf{K}(\mathbf{d}_{i-1})$ and $\mathbf{f}_{\text{int}}(\mathbf{d}_{i-1})$ have already been calculated during the previous step, and we solve for \mathbf{d}_i at load level \mathbf{f}_{ext} using

$$\mathbf{d}_i = \mathbf{d}_{i+1} + \Delta\mathbf{d}_i \quad (1.09)$$

One step of NR method is illustrated in Figure 6.

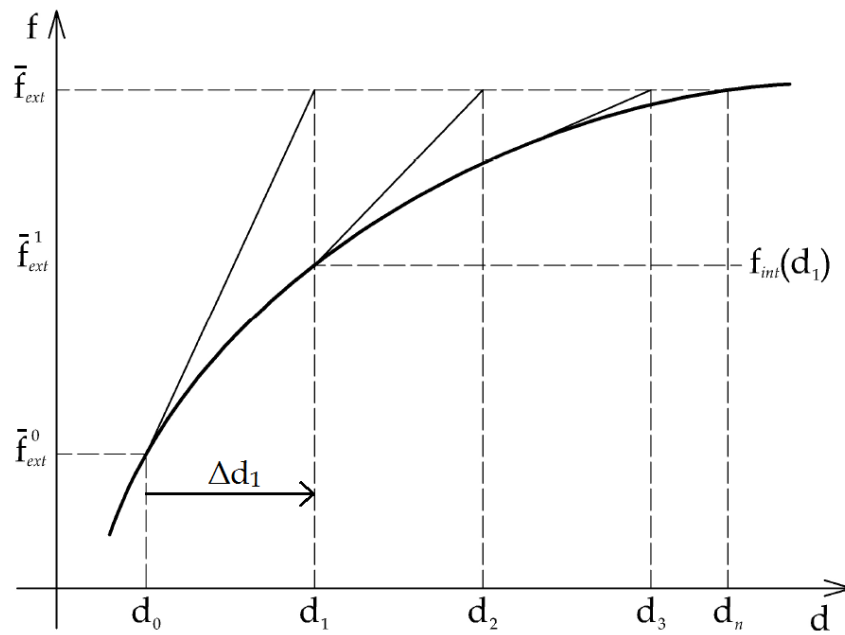


Figure 6 - Illustration of one step in Newton-Raphson method [11].

It is important to note that the stiffness matrix \mathbf{K} is updated in each iteration. This results in a rapid convergence, requiring less iterations.

An issue are the convergence criteria, i.e. the criteria for terminating the iteration cycles. That means that we need to define the conditions under which we can consider the approximate solutions for sufficiently close to equilibrium. There are three major criterions:

1. Criterion of increment displacements
2. Energy criterion
3. Criterion of unbalanced residues

The 1st criterion is most commonly used in FEM packages and it is defined as:

$$\frac{\|\Delta d^{(i)}\|_2}{\|{}^{t+\Delta t}d\|_2} \leq \varepsilon_D \quad (1.10)$$

where ε_D is called the convergence tolerance. It's a norm of displacement vector increment during iteration and it's small enough in comparison with the norm of vector total displacement at the end of the iteration [14].

2 Summary of the Theory of Elasticity

Displacement, strain and stress fields are cornerstones of the governing equations of elasticity. For the first they are valid if the structure undergoes small deformations only. Second condition is the linearity elastic manner of the material. Overall scheme of the system can be found on the Figure 7.

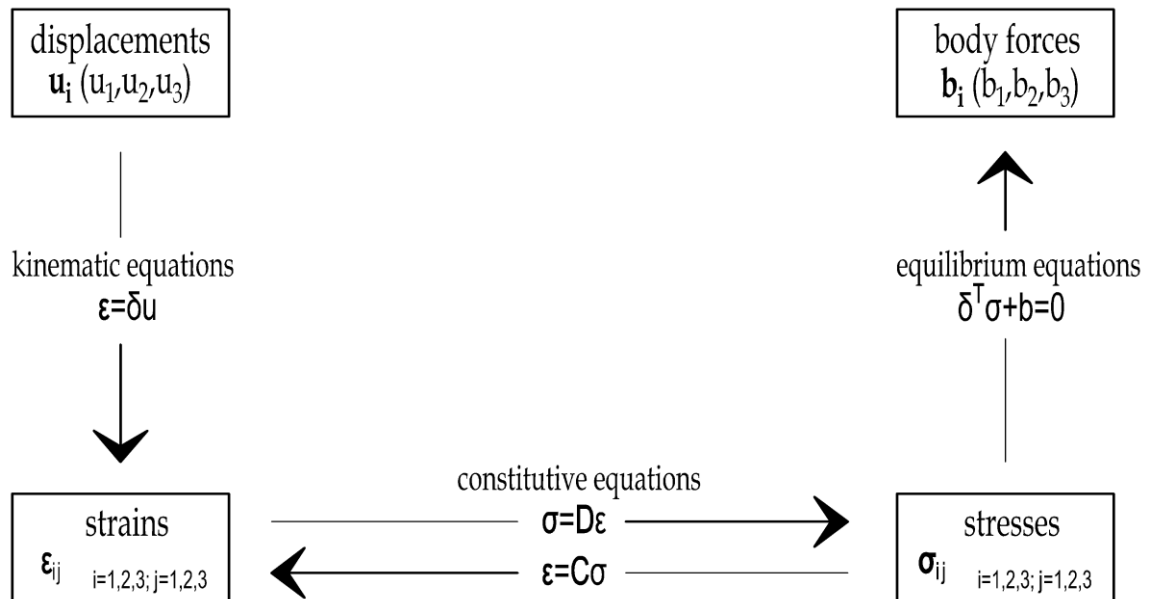


Figure 7 - Diagram of the kinematics and static equations.

2.1 Strain-to-Displacement Relations

2.1.1 Displacements

A displacement field is an assignment of displacement vectors for all points in a region or body that is displaced, or deformed, from one state to another. The displacements at each point is described by three components (u_1, u_2, u_3) , all of them dependent on the position in the Cartesian coordinate system (x_1, x_2, x_3) . In a matrix, the displacement vector can be written as

$$\mathbf{u} = [u_1, u_2, u_3]^T \quad (2.01)$$

where individual components of \mathbf{u} are functions of spatial coordinates i.e.

$$u_i = u_i(x_1, x_2, x_3) \quad (2.02)$$

2.1.2 Strains

In the following sections the attention will be focused on 2D problems only, but the transition to 3D problem is usually analogous and can be found in literature. Strain is a normalized measure of deformation representing the displacement between particles in the body relative to a reference length. In the infinitesimal strain (also called engineering strain) theory the stretching in the x-direction can be seen as the differential displacement per unit length. The x-component of strain is

$$\varepsilon_x = \lim_{\Delta x \rightarrow 0} \frac{\Delta u(x, y, z)}{\Delta x} = \frac{\partial u_1}{\partial x_1} \equiv \varepsilon_{11} \quad (2.03)$$

and it can be understood as a displacement gradient.

The engineering shear strain, or the change between two originally orthogonal lines is defined as

$$\gamma_{xy} = \alpha + \beta \approx \tan \alpha + \tan \beta = \frac{\partial u_1}{\partial x_2} + \frac{\partial u_2}{\partial x_1} \equiv 2\varepsilon_{12} \quad (2.04)$$

For the other components of strain tensor (ε_{22} , ε_{21}) the relationship between strain and displacement can be expressed analogously, yielding

$$\boldsymbol{\varepsilon} = \begin{bmatrix} \varepsilon_{11} & \varepsilon_{12} \\ \varepsilon_{21} & \varepsilon_{22} \end{bmatrix} = \begin{bmatrix} \frac{\partial u_1}{\partial x_1} & \frac{1}{2} \left(\frac{\partial u_1}{\partial x_2} + \frac{\partial u_2}{\partial x_1} \right) \\ \frac{1}{2} \left(\frac{\partial u_1}{\partial x_2} + \frac{\partial u_2}{\partial x_1} \right) & \frac{\partial u_2}{\partial x_2} \end{bmatrix} \quad (2.05)$$

2.2 Static Equations

Determining the variation of the stress components as functions of position within the interior of a body is obviously a principal goal in the stress analysis. The force equilibrium on an infinitesimal square results in the following Cauchy's equations:

$$\begin{aligned} \frac{\partial \sigma_{11}}{\partial x_1} + \frac{\partial \sigma_{12}}{\partial x_2} + b_{x_1} &= 0 \\ \frac{\partial \sigma_{21}}{\partial x_1} + \frac{\partial \sigma_{22}}{\partial x_2} + b_{x_2} &= 0 \end{aligned} \quad (2.06)$$

Based on the moment equilibrium on the infinitesimal square, we obtain:

$$\sigma_{12} = \sigma_{21} \quad (2.07)$$

Due to this fact the stress tensor is also symmetric.

Equilibrium of the stress and surface traction can be expressed by Cauchy's formula

$$\mathbf{t} = \lim_{\Delta A \rightarrow 0} \frac{\Delta \mathbf{F}}{\Delta A} \quad (2.08)$$

where \mathbf{t} is a traction vector, $\Delta \mathbf{F}$ external force and ΔA is the magnitude of the area on which $\Delta \mathbf{F}$ acts. Traction is a vector of the forces per area applied at the body surface and it is completely defined by two components (in 2-D) vectors associated with the coordinate planes.

Generally, for an arbitrary normal plane n it holds that

$$\mathbf{t}^{(n)} = \mathbf{t}^{(x)} n_x + \mathbf{t}^{(y)} n_y \quad (2.09)$$

which can be written in a compact form as:

$$\mathbf{t} = \boldsymbol{\sigma} \mathbf{n} \quad (2.10)$$

and in the index notation as:

$$t_j^{(n)} = \sigma_{ij} n_i \quad (2.11)$$

where n_i is a multiple of the cosine angle between the investigated plane and coordinate system (it is a projection onto the coordinate axes).

2.3 Constitutive Equations

Previous two sections were dealing with the kinematics (geometry) and static equilibrium of the body. When deriving the geometric equations it was assumed that the body is a continuum. This assumption is purely geometrical and does not provide anything about the role of material itself. In order to formulate the relationship between stress and strain tensors i.e. to develop the constitutive equations - we also assume that the material is homogenous and isotropic. Generally applied load in the 2D model we describe a stress-state by the three independent components of stress tensor related to the three components of the strain tensor, for convenience arranged in a column array as follows:

$$\boldsymbol{\sigma} = \begin{Bmatrix} \sigma_{11} \\ \sigma_{12} \\ \sigma_{22} \end{Bmatrix} \quad \boldsymbol{\varepsilon} = \begin{Bmatrix} \varepsilon_{11} \\ \varepsilon_{12} \\ \varepsilon_{22} \end{Bmatrix} \quad (2.12)$$

Sorting components of stress and strain is equivalent to each other and their dot product

$$\sigma^T \varepsilon = \sigma_{11}\varepsilon_{11} + \sigma_{12}\varepsilon_{12} + \sigma_{22}\varepsilon_{22} \quad (2.13)$$

has the meaning of the work done by the stress on deformations. In the linear theory of elasticity and assuming the material isotropy the relationship between stress and strains can be expressed by means of two independent constants, e.g. Young's modulus E and Poisson's ratio ν . Other constant, such as shear modulus G , can be expressed with previous two as follows

$$G = \frac{E}{2(1+\nu)} \quad (2.14)$$

The stresses and strains inside a continuous isotropic body are connected by a linear relationship also known as the Hooke's law. Basics expression for uniaxial stress is

$$\sigma = E\varepsilon \quad (2.15)$$

In two dimensions, it is useful to utilize the symmetry of stress and stress tensors, and to exploit the arrangement of the components to the column arrays (Voigt-Mandel notation). The stress-strain relationship can be then expressed as

$$\begin{Bmatrix} \sigma_{11} \\ \sigma_{12} \\ \sigma_{22} \end{Bmatrix} = \mathbf{D} \begin{Bmatrix} \varepsilon_{11} \\ \varepsilon_{12} \\ \varepsilon_{22} \end{Bmatrix} \quad (2.16)$$

where \mathbf{D} is the stiffness matrix described in the following section.

In two dimensional, sometimes called as plane theory of elasticity, we distinguish the following two general types of analysis: plane-stress and plane-strain, explained in the following sections.

2.3.1 Principal Stresses

When the coordinate system changes, the stress and strain components are changed too. That is the reason why there is an important role of invariants of stresses. Invariants of stress are suitably defined variables being independent on the coordinate system. These are called principal stresses and they are calculated for plane-stress problems as the roots of the following characteristic equation

$$\det \begin{bmatrix} \sigma_{11} - \sigma_1 & \sigma_{12} \\ \sigma_{21} & \sigma_{22} - \sigma_2 \end{bmatrix} = 0 \quad (2.17)$$

yielding

$$\sigma_{1,2} = \frac{\sigma_{11} + \sigma_{22}}{2} \pm \sqrt{\left(\frac{\sigma_{11} - \sigma_{22}}{2}\right)^2 + \sigma_{12}^2} \quad \sigma_3 = 0 \quad (2.18)$$

Similar way leads to obtaining the main invariants of strain tensor.

2.3.2 Plane-Stress

Plane-stress is defined to be a state of stress in which the normal stress, σ_{33} , and the shear stresses, σ_{13} and σ_{23} , directed perpendicular to the investigated plane are assumed to be zero. The geometry of the body is essentially that of a plate with one dimension much smaller than the others and the loads are applied uniformly over the thickness of the plate and act in the plane of the plate. The plane-stress condition is frequently encouraged in practice.

For isotropic materials and assuming

$$\sigma_{33} = \sigma_{13} = \sigma_{23} = 0 \quad (2.19)$$

and

$$\varepsilon_{13} = \varepsilon_{23} = 0 \quad (2.20)$$

yields

$$\sigma = \mathbf{D} \varepsilon \quad (2.21)$$

where

$$\mathbf{D} = \frac{E}{1-\nu^2} \begin{bmatrix} 1 & \nu & 0 \\ \nu & 1 & 0 \\ 0 & 0 & \frac{1-\nu}{2} \end{bmatrix} \quad (2.22)$$

is the material stiffness matrix. Similarly the dependence of strains on the stress can be expressed by the inversion of the previous equations, obtaining:

$$\varepsilon = \mathbf{C} \sigma \quad (2.23)$$

where

$$\mathbf{C}^{-1} = \mathbf{D} \quad (2.24)$$

we can obtain the non-zero out-of-plane deformation as

$$\varepsilon_{33} = -\frac{\nu}{E} (\sigma_x + \sigma_y) \quad (2.25)$$

2.3.3 Plane-Strain

Plane-strain is defined to be a state of strain in which the strain normal to the investigated plane, ε_{33} , and the shear strains ε_{13} and ε_{23} are assumed to be zero.

For isotropic materials and assuming

$$\varepsilon_{33} = \varepsilon_{13} = \varepsilon_{23} = 0 \quad (2.26)$$

and

$$\sigma_{13} = \sigma_{23} = 0 \quad (2.27)$$

$$\sigma = \mathbf{D} \varepsilon \quad (2.28)$$

where

$$\mathbf{D} = \frac{E}{(1+\nu)(1-2\nu)} \begin{bmatrix} 1-\nu & \nu & 0 \\ \nu & 1-\nu & 0 \\ 0 & 0 & \frac{1-2\nu}{2} \end{bmatrix} \quad (2.29)$$

and the out-of-plane stress can be then calculated as

$$\sigma_{33} = \frac{E}{1+\nu} \left[\frac{\nu}{1-2\nu} (\varepsilon_{11} + \varepsilon_{22}) \right] \quad (2.30)$$

3 Damage Model

Instead of the words elasticity, plasticity or fracture, which are used in real life with the same consequences like in mechanics. Usage of the word damage is very wide. In this text, we will focus to specify damage in narrow sense like a reduction of the internal integrity of a material caused by the creation, dissemination small cracks, voids and similar defects.

3.1 Isotropic Damage Model

A simple class of isotropic damage model is based on the stress-strain equation in the form [15]

$$\sigma = (1 - \omega) \mathbf{D} \varepsilon \quad (3.01)$$

where ω is a scalar damage variable, representing the rate of damage and evolving from 0 for the undamaged material and 1 for fully damaged material. Let assume new variable, called equivalent strain, $\tilde{\varepsilon}$, that depends on the strains ε . The maximum level of equivalent strain plays the role of internal variable, denoted as κ , representative maximum level of strain achieved during the "life" of material till the present t

$$\kappa(t) = \max_{t' \leq t} \tilde{\varepsilon}(t') \quad (3.02)$$

where t' running through the all times before the time t .

Course of the damage can be characterized as so-called damage law meantime understood as a dependency of damage parameter on deformation, which we can write as

$$\omega = g(\kappa) \quad (3.03)$$

where g is an function that is closely connected with the shape of stress-strain diagram. κ is formally described by the loading-unloading functions

$$f(\varepsilon, \kappa) \leq 0, \quad \kappa \geq 0, \quad \kappa f(\varepsilon, \kappa) = 0 \quad (3.04)$$

with the damage loading function defined as

$$f(\varepsilon, \kappa) = \tilde{\varepsilon}(\varepsilon) - \kappa \quad (3.05)$$

For example, setting $\tilde{\varepsilon}$ equal to the norm of the strain tensor, $\|\varepsilon\|$, we obtain a model with the same behaviour in tension and in compression, which is not suitable for quasi brittle materials with damage due to cracking.

A most popular formula for equivalent strain, proposed by Mazars, is based on the norm of the positive part of the strain tensor

$$\tilde{\varepsilon}(\boldsymbol{\varepsilon}) = \|\langle \boldsymbol{\varepsilon} \rangle\| = \sqrt{\sum_{I=1}^3 \langle \varepsilon_I \rangle^2} \quad (3.06)$$

where ε_I , with $I=1,2,3$, are the principal strains and their calculation was shown in previous section.

3.2 Material Softening

Many materials exhibits, when a certain measure of strain rate exceeds an elastic threshold, the process of softening. It means that with an increasing deformation stress decreases, which progressive softening is characteristic especially for quasi-brittle materials such as concrete. Softening curves of quasi-brittle materials are usually characterized by a relatively steep descent after the peak and by a long tail. In brittle materials there is present sudden crack growth, so the stress disappears almost immediately.

3.2.1 Linear Softening

For explanation, let us assume simple model as shown in Figure 8, where the stress-strain diagram is composed of two linear curves. One curve represents elastics behavior and the second one linear softening. Material is elastics till the limit strain, denoted as ε_0 , is reached. Stress transmitted by material completely disappears at ultimate strain, denoted ε_f .

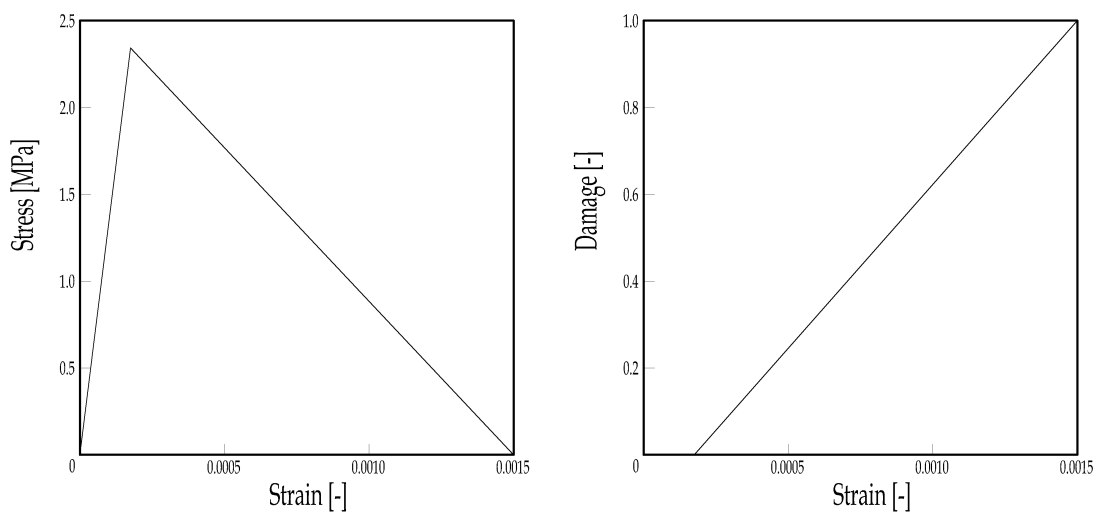


Figure 8 - Stress-strain diagram with linear softening (left) and the corresponding dependence of damage on strain (right).

3.2.2 Exponential Softening

When the equivalent strain, such as Mazars norm [17], exceeds the elastic limit, the microcracking occurs and the softening takes place. This is advancing if any new maximum of the equivalent strain reached. The maxima are stored in the internal variable Kappa, κ , meaning "historically the maximum reached value of equivalent strain at a given point". The softening part of the stress-strain diagram can be approximated by a non-linear law, or by a bilinear softening law with a low knee point [15].

Let us consider a simple damage law characterized by an exponential softening (Figure 9)

$$\omega = g(\kappa) \equiv \begin{cases} 0 & \text{for } \kappa \leq \varepsilon_0 \\ 1 - \frac{\varepsilon_0}{\kappa} \exp\left(-\frac{\kappa - \varepsilon_0}{\varepsilon_f - \varepsilon_0}\right) & \text{for } \kappa > \varepsilon_0 \end{cases} \quad (3.08)$$

where ε_0 is the limit elastic strain (Hooke's law validity) up to the peak, followed by exponential softening, when $\kappa > \varepsilon_0$. The stress transmitted by the material can be expressed as a function of strain as follows

$$\sigma(\varepsilon) = [1 - g(\varepsilon)] E \varepsilon = \begin{cases} E \varepsilon & \text{for } \varepsilon \leq \varepsilon_0 \\ E \varepsilon_0 \exp\left(-\frac{\varepsilon - \varepsilon_0}{\varepsilon_f - \varepsilon_0}\right) & \text{for } \varepsilon > \varepsilon_0 \end{cases} \quad (3.09)$$

where parameter ε_f controls the slope of softening diagram, as shown in Figure 9.

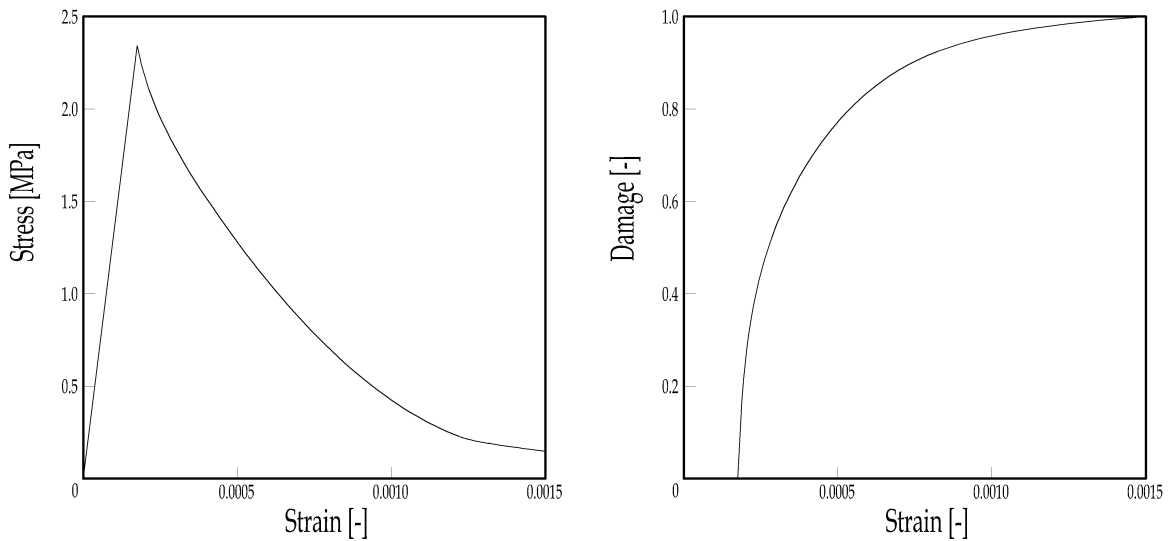


Figure 9 - Stress-strain diagram with exponential softening (left) and the corresponding dependence of damage on strain (right).

The area under the stress-strain diagram, defined as

$$g_f = \int_0^{\infty} \sigma(\varepsilon) d\varepsilon = E\varepsilon_0 \left(\varepsilon_f - \frac{\varepsilon_0}{2} \right) \quad (3.10)$$

and represents the energy dissipated per unit volume at complete failure. It is closely related to the fracture energy of the material G_f . For a continuum damage model with damage localized into a band of width h_b , we obtain

$$G_f = h_b g_f \quad (3.11)$$

3.2.3 Damage Localization

In numerical calculations, when utilizing the softening law, the results exhibit a pathological sensitivity to discretization parameters such as the element size in the simulation. It is well known that softening can induce localization of inelastic processes into zones arbitrary small thickness. This is rendered by using the "global criteria" defining the fracturing threshold, such as maximum cohesive crack thickness, fracture energy, or using the non-local formulation of the damage laws [17].

PART II:
CALCULATIONS

4 Calculations

The purpose of FEA was simulation of performed experiments, it should have just indicated the trends and shown the failure mechanism. This approach is much more time and cost efficient compared to an old-fashioned purely experimental analysis. The simulations were focused on the investigation of aggregate shape, size and material influence on the bending strength evaluated from three-point bending tests, and fracture-mechanical properties evaluated from a series of splitting tests.

4.1 Steps of Calculation

The modern commercial package enables to perform all steps of FE modeling such as model preparation, meshing, setting of boundary conditions, calculating and displaying results. Free academic packages are often focused on a single issue, but compared to the commercial ones they provide very efficient and advanced functions. Therefore, different software packages are often used for individual steps. In our case, the FE modeling was accomplished in the following steps:

- geometry preparation using MATLAB
- meshing in ANSYS
- FE calculation by OOFEM
- plotting stress-strain diagrams in MATLAB
- postprocessing and featuring the graphical outputs in PARAVIEW

4.2 Geometry of Tested Specimens

The geometry of tested specimens is specified by Figure 10 and 11.

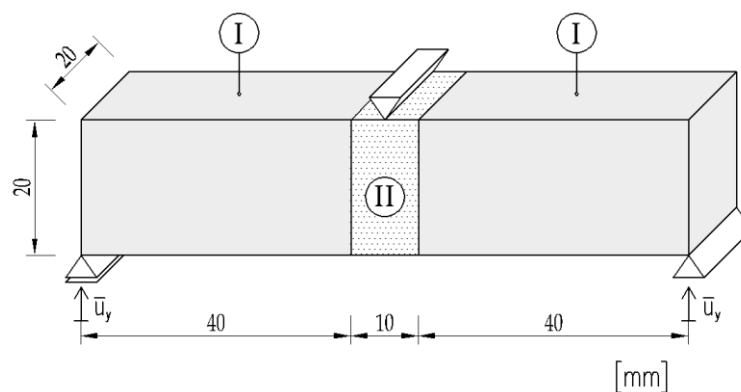


Figure 10 - Geometry of tested specimen - bending test.

The aggregates of round, ellipsoidal and angular shape were placed only in the area of expected crack propagation, area is labeled as II, in a relative volume $c_{agg}=0.4$. Each aggregate shape configuration was represented by the fine (F) (passing

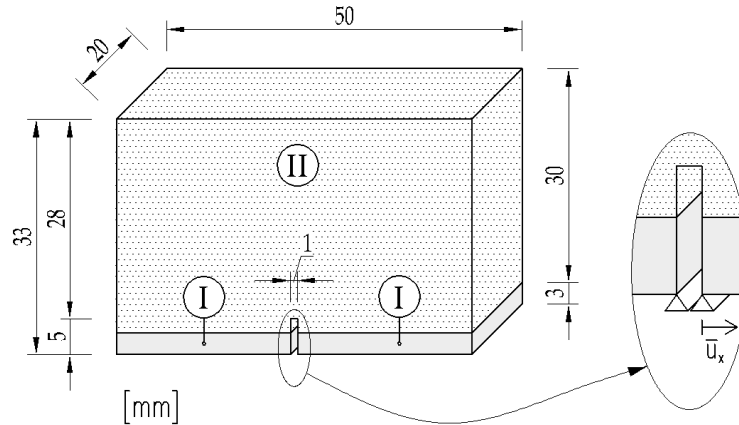


Figure 11 - Geometry of tested specimen - splitting test.

the sieve opening $d_0 = 1.0$ mm) and coarse (C) ($d_0 = 2.5$ mm) monodisperse particles. The individual aggregate configurations are summarized in the Table 1.

Table 1 - Summary of simulated aggregate configurations

	code	shorter semi-axis [mm]	longer semi-axis[mm]
angular coarse aggregates	A(C)	2.5	5
angular fine aggregates	A(F)	1	2
ellipsoid coarse aggregates	E(C)	2.5	5
ellipsoid fine aggregates	E(F)	1	2
round coarse aggregates	R(C)	2.5	2.5
round fine aggregates	R(F)	1	1

The procedure of the geometry generation was implemented in MATLAB software and the MPT toolbox for MATLAB [16] was used for the generation of the aggregates.

For meshing triangular elements were used. The conforming finite element mesh was generated with the ANSYS software. Mesh density was coarse near the supports and greatly refined in the expected area of crack propagation. Examples of the fine-meshed area during the bending test and meshed model for splitting test are shown in Figure 12.

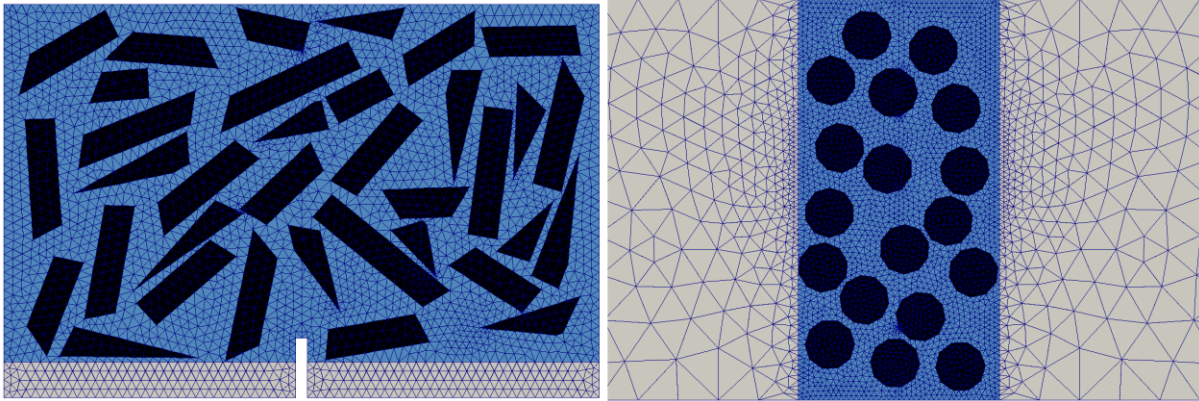


Figure 12 – Meshed model for splitting test (left) and mesh in middle part for bending test (right).

4.2.1 Principles Used for Generation of Aggregates

Aggregates were generated with random orientation and distribution using the toolbox for MATLAB [16]. The randomness ensured the statistical validity of obtained results. On the other hand, positioning was restricted by following conditions:

- aggregates cannot cross the specimen boundaries (i.e. modeled as if cast, non-periodic boundary)
- the notch could not be entirely blocked by the bridging aggregate (Figure 13)

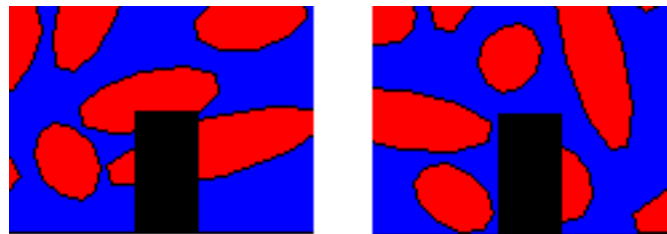


Figure 13 – Bad distribution of aggregates around notch (left), satisfying distribution of aggregates around notch (right)

4.3 Finite Element Calculation

The plane-stress numerical simulations were carried out in the OOFEM finite element code with the object oriented architecture [7]. An isotropic damage model with linear softening [17] was assumed for the matrix phase, while the aggregates were modeled as isotropic and elastic. The equivalent strain, $\tilde{\varepsilon}$, was determined based on Mazars norm (Equ. 3.05), accounting only for the positive part of the strain tensor. The interfacial transition zone was not modeled. The material properties of the matrix and aggregates are summarized in the Table 2. The input parameters were: Young's modulus, E , Poisson's ratio, ν , and in case of matrix also strain at peak stress ε_0 and crack opening at complete failure w_f . In order to avoid damage around nodes with controlled displacement, the loaded and supported areas were also

modeled as isotropic elastic material, having the stiffness of the homogenized material (denoted "homogenized regions" in Table 2; 1-for bending and splitting test with sand aggregates, 2-bending test with bricks aggregates) characterized by elastic constants obtained using Mori-Tanaka scheme [18, 19].

Table 2 – Material properties of individual phases.

	E [GPa]	ν [-]	ϵ_0 [-]	w_f [μm]	notes
matrix	3,2	0.2	0.0004	1	brittle material, linear softening
sand aggregates	60	0.2	∞	∞	elastic material
brick aggregates	8	0.2	0.000425	1	elastic material
homogenized regions 1	9	0.2	∞	∞	elastic material
homogenized regions 2	4,5	0.2	∞	∞	elastic material

The matrix phase was represented by a brittle lime-based paste and its properties were determined from experiments [20], while the properties of aggregates were determined based on the literature study [21, 22].

4.3.1 Summary of Tested Specimens

Six random distribution per each of six aggregate shape and size configurations were generated. The samples with crushed brick aggregate, which was assumed to be angular, are denoted as "br". The studied configurations are summarized in Table 3.

Table 3 – Summary of tested aggregate configurations.

BENDING		SPLITTING	
A(C)	A(C,br)	A(C)	A(C,br)
A(F)	A(F,br)	A(F)	A(F,br)
R(C)		R(C)	
R(F)		R(F)	
E(C)		E(C)	
E(F)		E(F)	

4.4 Stress-strain Diagrams

Stress-strain diagrams for each configuration have been made as averaged stress-strain diagrams of all six tested specimens. Averaged values were Young's modulus E , tensile strength f_t and for splitting test, where the softening part of the diagram was approximated with an exponential function, also the averaged fracture energy G_f was used to find an equivalent average diagram. Because of the unstable crack propagation and presence a snapback² phenomenon, the bending test could not be used for the evaluation of fracture energy. Some examples of diagrams are shown in Figure 13, 14 and 15.

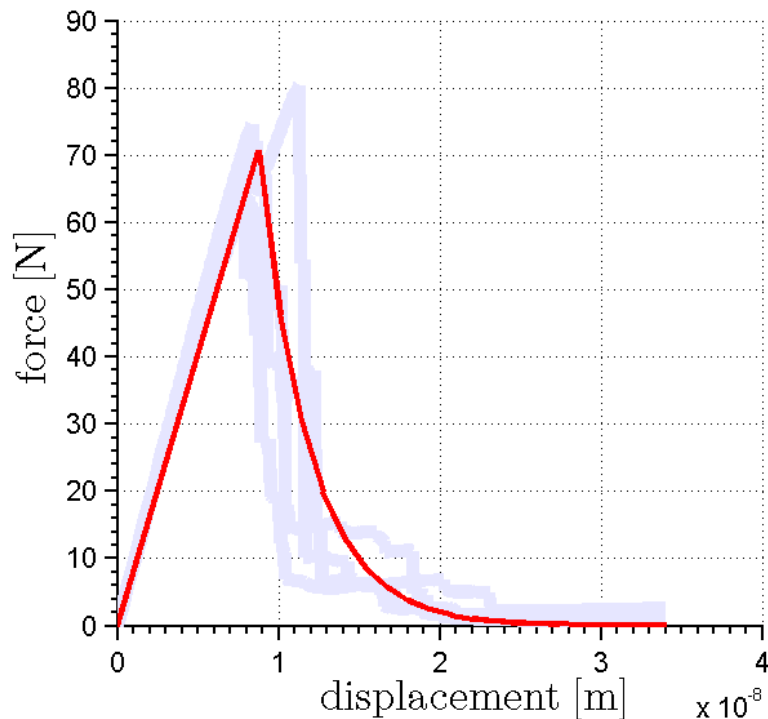


Figure 13 - Averaged stress-strain diagram for splitting test A(F).

² For extremely brittle materials, the snapback in the equilibrium path occurs and the load-displacement softening branch assumes a positive slope. Both load and displacement must decrease to obtain slow and controlled crack propagation (whereas in normal softening only the load must decrease). If the loading process is displacement-controlled, the loading capacity presents a discontinuity with a negative jump. It is caused by catastrophic decrease of stiffness at initialization of crack propagation process [23, 24].

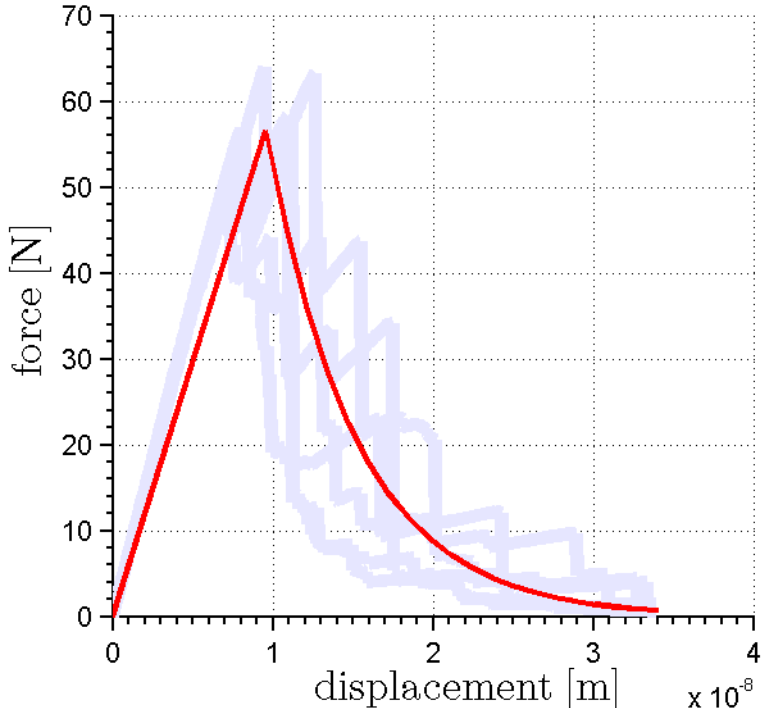


Figure 14 - Averaged stress-strain diagram for splitting test A(F, br).

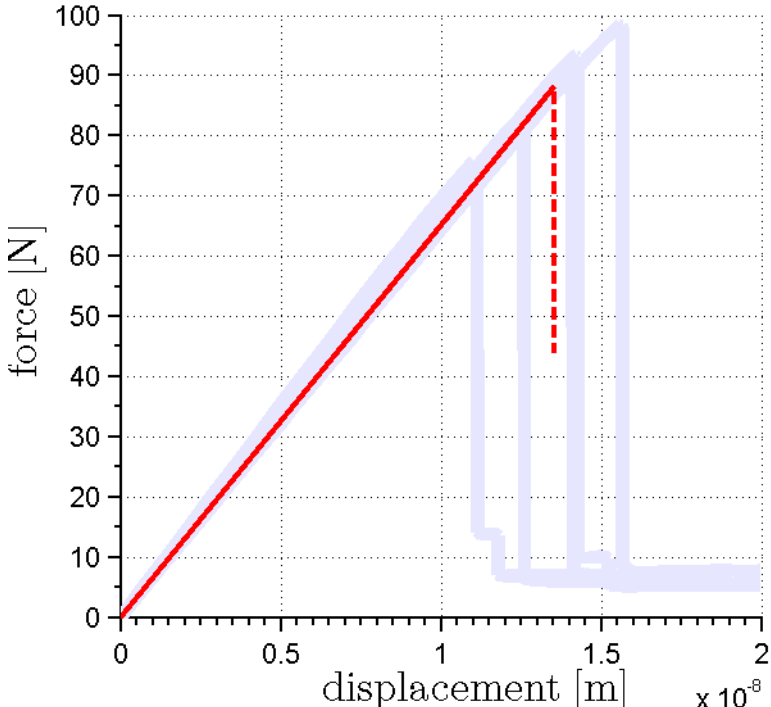


Figure 15 - Averaged stress-strain diagram for bending test R(C).

4.5 Postprocessing

Postprocessing, and graphical illustration of outputs such as crack propagation, stress, strain or displacement were carried out using PARAVIEW software [25]. Some examples of graphical outputs are shown in Figure 16 and 17.

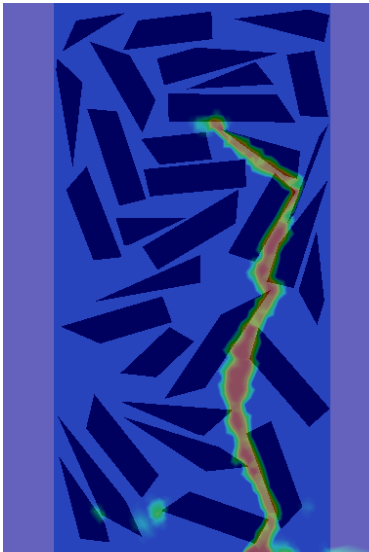


Figure 16 - Crack propagation during bending test A(C, br)_5.

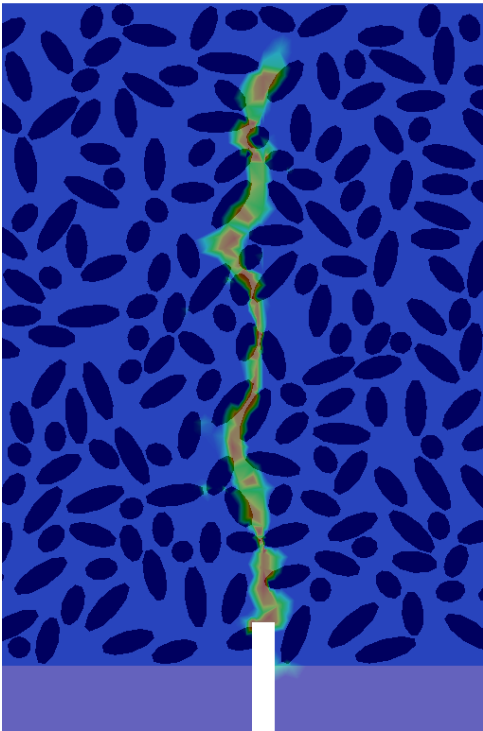


Figure 17 - Crack propagation during splitting test E(F)_6.

5 Results and Discussion

5.1 Bending Test

Results of bending tests were averaged within the individual configurations, providing a smooth force-displacement diagram. Resulting comparison providing information about the aggregate shape influence on mortar bending strength is shown in Figure 18.

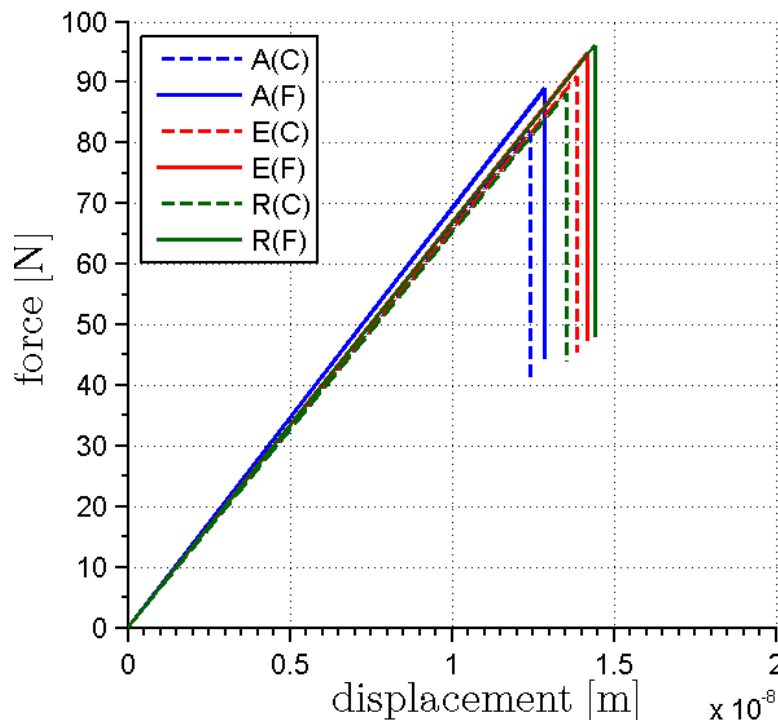


Figure 18 - Averaged load-displacement diagrams for individual aggregate configurations.

The stress concentrations due to presence of angular particles resulted in a lower resistance of the specimens in three-point bending tests, which was even more pronounced in case of beams containing coarse particles. On the other hand, the fine round particles resulted in the highest bending strength. The stiffness of the specimens was not significantly influenced by the shape of the particles and the slight deviations were caused by the variable arrangement of the the particles within the sample.

In Figure 19 the influence of crushed brick aggregates on the mortar mechanical properties is demonstrated. The results clearly indicate that the use of crushed bricks particles increases the ductility of tested specimens. The fracture energy of the mortars containing crushed brick particles, determined from the three-point bending test, was also increased, compared to the mortars containing sand.

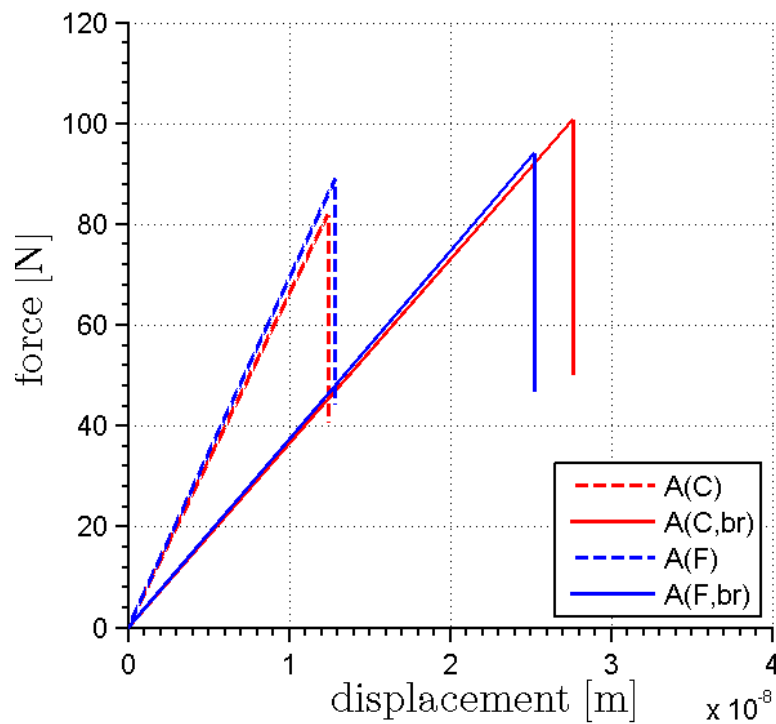


Figure 19 - Averaged load-displacement diagrams for angular configuration of sand and brick aggregates.

In Table 4, the numerical values obtained during the bending test, in particular maximum force F_{\max} , corresponding maximum displacement at $u_{y,\max}$ are summarized.

Table 4 - Results of three-point bending test simulations.

codename	F_{\max} [N]	$u_{y,\max}$ [$\times 10^{-8}$ m]
A(C)	81.9	1.24
A(C,br)	100.8	2.76
A(F)	89.0	1.29
A(F,br)	94.1	2.52
E(C)	90.9	1.38
E(F)	94.7	1.42
R(C)	88.1	1.35
R(F)	96.1	1.44

5.2 Splitting Test

Results of splitting tests were averaged within the individual configurations, providing a smooth force-displacement diagram. Result comparison of aggregate shape influence is shown in Figure 20. The softening part had to obey the mean value of the energy dissipated during the simulations, and it was approximated by an exponential curve.

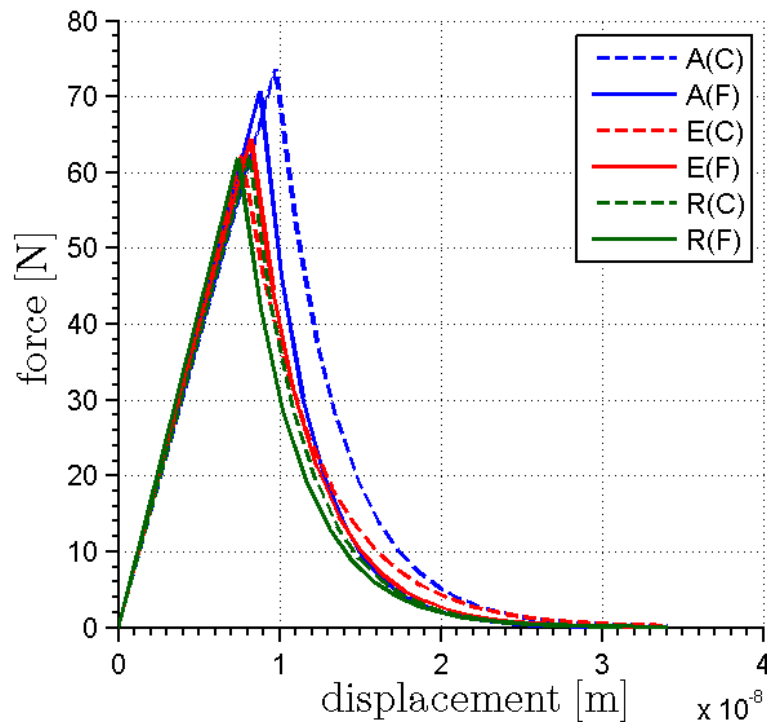


Figure 20 - Averaged load-displacement diagrams for individual aggregate configurations.

The opposite trends were observed in splitting than in bending simulations, where the coarse angular aggregates contributed to higher fracture energy of the mortar, while the round aggregates enabled relatively easy crack propagation through the specimens. Material influence of brick particles is demonstrated in Figure 21. The results indicate the same trend, which was observed in the bending test, that the elastic deformation of mortars containing crushed brick particles is increased.

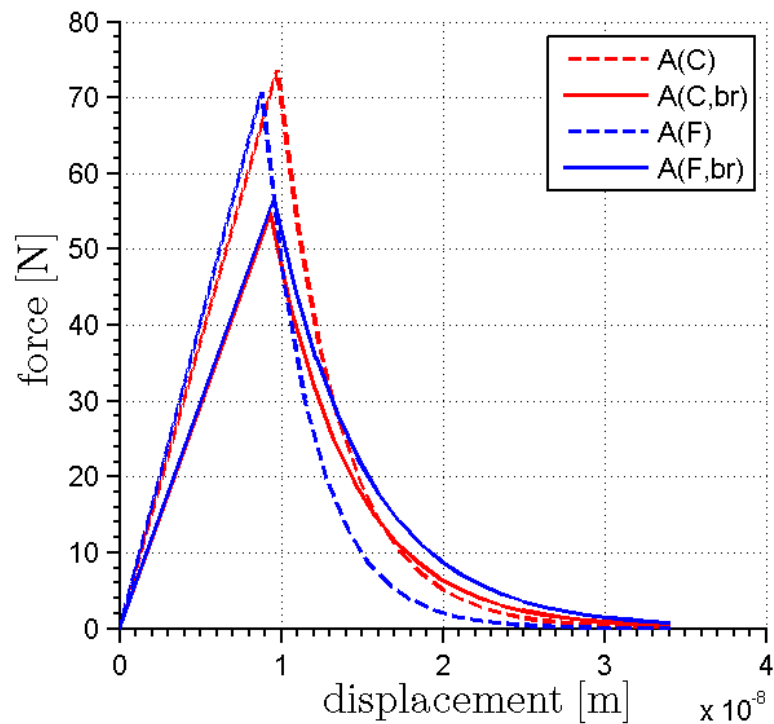


Figure 21 - Averaged load-displacement diagrams for angular configuration of sand and brick aggregates.

In Table 5 are summarized numerical values obtained during the splitting test. Values are: maximum force F_{\max} , corresponding maximum displacement at F_{\max} and value of work that is needed to fracture the beam, G_f , called fracture energy.

Table 5 - Results of three-point bending test simulations.

codename	F_{\max} [N]	$u_{y,\max}$ [$\times 10^{-9}$ m]	G_f [$\times 10^{-7}$ J]
A(C)	73.6	9.74	6.43
A(C,br)	54.8	9.33	5.26
A(F)	70.7	8.76	5.36
A(F,br)	56.6	9.56	5.83
E(C)	62.3	7.63	5.25
E(F)	54.5	8.21	5.04
R(C)	62.1	8.11	4.74
R(F)	61.9	7.43	4.56

Conclusion

The present work was focused on the influence of aggregates embedded in the brittle matrix, represented by the isotropic damage model with linear softening. In particular, the bending strength and fracture-mechanical properties were evaluated from the finite element simulations of bending and splitting tests. The following conclusions can be made from the results of the analysis:

- 2D plane-stress finite element simulations and isotropic damage model can successfully simulate the crack propagation through a microstructure in a realistic way,
- simulation of splitting test can be used for the evaluation of fracture energy in brittle materials without snap-back response in load-displacement diagram,
- the bending strength is enhanced by the addition of fine spherical sand particles into mortars, since they do not introduce excessive stress concentrations around their tips,
- the fracture energy of mortars can be enhanced by the addition of coarse angular aggregates, since these create an efficient obstacle against the crack propagation,
- the maximum elastic strain of mortars containing crushed bricks is much higher compared to those containing sand aggregates only,
- the stress concentration near the brick aggregates boundaries are reduced and the crack is often forced to pass through the crushed brick particle which results in an additional energy dissipation.

The study was not supposed to yield exact values, it only revealed the trends. Three-dimensional model, incorporating shrinkage micro-cracking and interfacial zone around aggregates, would probably give more accurate data at significantly higher computational cost.

References

- [1] STEFANIDOU, M. and PAPAYIANNI, I. (2005). *The role of aggregates on the structure and properties of lime mortars*. *Cement & Concrete Composites*, 27:914–919.
- [2] TASONG, W., LYNSDALE, C. and CRIPPS, J. (1998). *Aggregate-cement paste interface: influence of aggregate physical properties*. *Cement and Concrete Research*, 28(10):1453–1465.
- [3] BARONIO, G., BINDA, L. and LOMBARDINI, L. (1997) *The role of brick pebbles and dust in conglomerates based on hydrated lime and crushed bricks*, *Construction and Building Materials* 11 33–40.
- [4] NEŽERKA, V. and ZEMAN, J. (2012) *A micromechanics-based model for stiffness and strength estimation of cocciopesto mortars*, *Acta Polytechnica* 52 29–37.
- [5] TANENBAUM, S. *Modern operating systems*. New Jersey: Prentice-Hall, 2001, 950 p. ISBN 01-303-1358-0.
- [6] Narasaiah, G. *Finite element analysis*. Hyderabad: BS Publications, 2008, 340 p. ISBN 978-81-7800-140-1.
- [7] PATZÁK, B. *OOFEM project home page*, <http://www.oofem.org>, 2000.
- [8] WIKIPEDIA, Available online at http://en.wikipedia.org/wiki/List_of_finite_element_software_packages
- [9] RAO, S. *The finite element method in engineering*. 4th ed. Boston, MA: Elsevier/ Butterworth Heinemann, 2005, XIX, 663 p. ISBN 0750678283.
- [10] GOKHALE, N., DESHPANDE, S., BEDEKAR, S. and THITE, A. *Finite to Infinite* (2008) ISBN 978-81-906195-0-9.
- [11] SOMR, M. *Numerical Simulation of Cocciopesto-based Masonry Structures*. Prague, 2012. Diploma thesis. FCE CTU in Prague.
- [12] ZEMAN, J. [online]. Prague. Available online at: <http://ksm.fsv.cvut.cz/~zemanj/teaching/mk10/prednasky/prednaska5.pdf>. Lecture notes. FCE CTU in Prague.
- [13] IVANČO, V. [online]. Košice. Available online at: http://www.mb.hs-wismar.de/~heinze/subdir/FEA_of_Nonlinear_Problems_2011_Ivanco.pdf. Lecture notes. FME TU Košice, 2011.

- [14] KABELE, P. [online]. Prague. Available online at: <http://people.fsv.cvut.cz/~pkabele/YNAK/Lecture notes>. FCE CTU in Prague.
- [15] JIRÁSEK, M. and BAUER, M. *Numerical aspects of the crack band approach*, Computers & Structures, Volumes 110–111, November 2012, Pages 60–78, ISSN 0045-7949, 10.1016.
- [16] KVASNICA, M. (2009). *Real-Time Model Predictive Control via Multi-Parametric Programming: Theory and Tools*. VDM Verlag, Saarbruecken.
- [17] JIRÁSEK, M. and ZEMAN J. *Přetvoření a porušování materiálů: dotvarování, plasticita, lom a poškození*. 2. edition. FCE CTU in Prague, 2012, 177 s. ISBN 978-80-01-05064-4.
- [18] MORI, T. and TANAKA, K. (1973). *Average stress in matrix and average elastic energy of materials with mixfitting inclusions*. Acta Metallurgica, 21:571–574.
- [19] BENVENISTE, Y. (1987). *A new approach to the application of Mori-Tanaka theory in composite materials*. Mechanics of Materials, 6:147–157.
- [20] NEŽERKA, V., SLÍŽKOVÁ, Z., TESÁREK, P., PLACHÝ, T., FRENKEOVÁ, D., and PETRÁŇOVÁ, V. (submitted 2013). *Comprehensive study on microstructure and mechanical properties of lime-pozzolan pastes*. Cement and Concrete Research.
- [21] SHARPE Jr., W., PULSKAMP, J., GIANOLA, D., EBERL, C., POLCAWICH, R., and THOMSON, R. (2007). *Strain Measurements of Silicon Dioxide Microspecimens by Digital Imaging Processing*. Experimental Mechanics, 47:649–658.
- [22] VOREL, J., ŠMILAULER, V. and BITTNAR, Z. *Multiscale simulations of concrete mechanical tests*, Journal of Computational and Applied Mathematics 236 (2012) 4882–4892.
- [23] AND MONETTO I. and CARPINTERI A. *Snap-back analysis of fracture evolution in multi-cracked solids using boundary element method*. International Journal of Fracture 98: 225–241, 1999.
- [24] CARPINTERI A., COLOMBO G. *Numerical analysis of catastrophic softening behaviour (snap-back instability)*. Computers & Structures. Volume 31, Issue 4, 1989, Pages 607–636.
- [25] HENDERSON, A. *ParaView Guide*. A Parallel Visualization Application. Kitware Inc., 2007.